[5] Wilson, W. K., "Some Crack Tip Finite Elements for Plane Elasticity," *Stress Analysis and Growth of Cracks: Proceedings of the 1971 National Symposium on Fracture Mechanics*, Pt. I, STP 513, Sept. 1971, pp. 90–105, American Society for Testing and Materials, Philadelphia, Pa.

[6] Pian T. H. H., Tong, P., and Luk, C. H., "Elastic Crack Analysis by a Finite Element Hybrid Method," *Proceedings of the Third Conference on Matrix Methods in Structural Mechanics*, Wright-Patterson Air Force Base, Ohio, 1971.

[7] Aberson, J. A. and Anderson, J. M., "Cracked Finite Elements Proposed for NASTRAN," *Proceedings of the NASTRAN User's Colloquium*, Sept. 1973.

[8] Hardy, R. H., "A High-Order Finite Element for Two-Dimensional Crack Problems," Ph.D. thesis, Georgia Institute of Technology, Atlanta, Ga., 1974.

[9] Williams, M. L., "On the Stress Distribution at the Base of a Stationary Crack," *Journal of Applied Mechanics*, Vol. 24, No. 1, March 1957, pp. 109–114.

[10] Sih, G. C., Embley, G. T., and Ravera, R. S., "Impact Response of a Plane Crack in Extension," *International Journal of Solids and Structures*, Vol. 8, No. 7, July 1972, pp. 977–993.

Numerical Solution of a Nonlinear Integral Equation by the Use of Step Functions: III. Continuous Solutions

KENNETH K. YOSHIKAWA*
NASA Ames Research Center, Moffett Field, Calif.

Nomenclature

A = matrix defined in Eq. (5)
B = integrated quantity of Planck's function, $\theta^4 I(z)$
E_n = exponential integral of order n
F = nondimensional boundary flux, or function of variable Ψ
f = boundary function defined in Eq. (3)
g = boundary function
h = Planck's constant
I = one-half the total step number, or

$$I(z) = 15/\pi^4 \int_0^\infty \delta(\alpha_\nu) z^3\, dz/(e^{-z}-1)$$

J = functional
K = kernel function
Ki = indefinite integral of the kernel function
k = Boltzmann's constant
M = number of iterations
N = number of spectral band

$$\text{sgn}\,(x) = \begin{cases} + \text{ if } x > 0 \\ - \text{ if } x < 0 \end{cases}$$

T = temperature, or integral of the kernel function, Eq. (9)
z = variable, $\bar{\nu}/\theta$
α = absorption coefficient
δ = delta function, $\delta(\alpha_\nu) = \begin{cases} 1 \text{ for frequencies where } \alpha_\nu = \alpha_k \\ 0 \text{ otherwise} \end{cases}$
Δ = constant increment in step function approximating the function Ψ
$\Delta\nu_k$ = increment of frequency, $\nu_{k+1} - \nu_k$
η = optical thickness, $-l \leqq \eta \leqq l$
$\bar{\eta}$ = dimensionless optical thickness, η/l
θ = normalized temperature, T/T_B
l = one-half the optical thickness
λ = constant in integral equation
ν = frequency
$\bar{\nu}$ = nondimensional frequency, $h\nu/kT_B$
σ = Stefan-Boltzmann constant
ϕ = variational function
Ψ = solution
ψ = step solution
τ_w = total optical thickness, $2l$

Subscripts

A = at one boundary
B = at the other boundary
I = at Ith point
i, j = indexes of summation, or at ith or jth step point
k = frequency interval corresponding to kth spectral band
ν = frequency

Superscript

$-$ = normalized

Received June 14, 1974.
Index categories: Rarefied Flows; Atmospheric, Space, and Oceanographic Sciences; Radiation and Radiative Heat Transfer.

* Aerospace Research Scientist, Thermogasdynamic Division. Member AIAA.

Introduction

INTEGRAL equations play an important role in the development of many problems in physics and fluid dynamics, e.g., in the boundary value problems involved in kinetic theory, in the radiative transfer equation, in wing theory, in Boltzmann's equation, and in Schrodinger's equation for the quantum theory of scattering. For problems that require numerical solutions involving complicated sets of boundary conditions, it may be more practical to obtain solutions rapidly with moderate accuracy than time consuming exact solutions. Such cases arise in the calculation of the transition probabilities for use in the Monte Carlo simulation of reacting flow and in the classical master equations for the nonequilibrium dissociation and recombination reactions, for example.

In previous studies,[1-3] the author has demonstrated the advantages of the step function incorporated with the variational technique. It is, however, often desirable to have a continuous solution, rather than the step function solution, especially near the boundary point where the values of solution change rapidly. This Note will demonstrate that accurate continuous solutions can be derived from the results of the previous step function solutions.

Analysis

Basic Equation

The basic nonlinear integral equation considered in the present problem may be written in symbolic notation as

$$F(\Psi) = g + \lambda K\Psi \tag{1}$$

where F is a given function of the unknown variable Ψ, g is the boundary function, λ is a given constant, and K is the symmetric singular kernel. (Here, we simply assume a unique solution exists.)

For the purpose of numerical calculation, Eq. (1) is recast into the standard form of Fredholm's equation (second kind)

$$\Psi = f + \lambda K\Psi \tag{2}$$

where

$$f = \Psi - F(\Psi) + g \tag{3}$$

The f function in Eq. (2) is treated as a known quantity since, in practice, an (arbitrary) initial guess for Ψ can be used.

A solution to the linear integral Eq. (2) is obtained by the variational method, which extremizes the functional J

$$J(\phi) = 1/2\,\|\phi\|^2 - 1/2(\lambda K\phi + 2f)\phi \tag{4}$$

The functional J takes a minimum value at $\phi = \Psi$, which is the solution of Eq. (2).

Step Function Solution

The function Ψ is approximated stepwise by a number I of constants

$$\Delta_i, \psi_i = \sum_{j=1}^{i} \Delta_j$$

Substituting these step constants into Eq. (4), and minimizing J with respect to Δ_i, the solution to Eq. (2) for known values of the f function is obtained

$$\frac{\partial J}{\partial \Delta_i} = \sum_{j=1}^{I} A_{ij}\Delta_j - A_i = 0, \qquad i = 1, 2, \ldots, I \tag{5}$$

where A_{ij} and A_i are matrices involving integrals of the kernel and boundary functions. The analysis pertaining to this method is described in Ref. 2. It is worthwhile to comment, however, that the A_{ij} and A_i can be evaluated given an initial f distribution. The Δ_j are then found by solving the above system of equations. This procedure is repeated in an iterative manner until convergence is obtained.

Continuous Solution

After the step-constant solution ψ_i has been obtained, one may calculate a continuous solution by substituting ψ_i directly into the right-hand side of Eq. (1). Since the function to be integrated along with the *singular* kernel function is a set of constants, this evaluation is simple and straightforward. The solution, piecewise analytic and continuous, can be written in symbolic notation as

$$\Psi = F^{-1}(g + \lambda K\psi) \tag{6}$$

Substitution of ψ_i into Eq. (6) yields

$$\Psi = F^{-1}\left(g + \lambda \sum_{j=1}^{2I} \Delta_j T_j\right) \tag{7}$$

where

$$T_j \equiv T(\eta, \eta_j) = \int_{\eta_j}^{l} K(|\eta' - \eta|)\, d\eta'$$
$$= \operatorname{sgn}(\eta_j - \eta)[-Ki(|\eta_j - \eta|) + Ki(0)] - Ki(l - \eta) + Ki(0) \tag{8}$$

and

$$\int_0^{\eta} K(\eta')\, d\eta' = Ki(\eta) - Ki(0) \tag{9}$$

For example, with the exponential integral as the kernel, $K(\eta) = E_1(\eta)$ it follows that $Ki(\eta) = -E_2(\eta)$.

Application

The following integral equation is applicable to dimensionless radiative transfer for planar-planetary atmosphere with spectral absorption coefficient, α_ν, of the Milne-Eddington type approximated by the "picket fence" model[2-4]

$$\sum_{k=1}^{N} \alpha_k B_k(\theta) = 1/2 \sum_{k=1}^{N} \left[\alpha_k F_{Ak} E_2(l_k + \eta_k) + \alpha_k F_{Bk} E_2(l_k - \eta_k) + \int_{-l_k}^{l_k} \alpha_k B_k(\theta) E_1 |\eta_k - \eta'| \right] d\eta' \tag{10}$$

where F_{Ak} and F_{Bk} are the boundary fluxes at layers A and B, respectively (see nomenclature for other symbols).

Equation (10) is solved in the manner described earlier by use of the step constants for the trial function in the variational method. Let the step solution ψ be represented by $B_k(\theta)$

$$B_k(\theta) = \sum_{i=1}^{j} (\Delta_k)_i \tag{11}$$

Then, in similar manner as before [Eqs. (7–9)], one may substitute the step solution B_k into the right-hand side of Eq. (10). The following result is then obtained:

$$\theta^4 \sum_{k=1}^{N} \alpha_k \Delta I_k(\theta) = \sum_{k=1}^{N} \left\{ g_k + \alpha_k/2 \sum_{j=1}^{I} (\Delta_k)_j T_{kj} \right\} \tag{12}$$

where

$$\Delta I_k(\theta) = I_k\{(\bar{\nu} + \Delta\bar{\nu})/\theta\} - I_k(\bar{\nu}/\theta)$$
$$g_k = \alpha_k/2\{F_{Ak} E_2(l_k + \eta_k) + F_{Bk} E_2(l_k - \eta_k)\}$$
$$T_{kj} = \begin{cases} E_2(\eta_k - \eta_{kj}) & \eta_{kj} \leqq \eta_k \\ 2 - E_2(\eta_{kj} - \eta_k) & \eta_{kj} > \eta_k \end{cases} \tag{13}$$

and $\Delta\bar{\nu}$ is the frequency interval for $\alpha_\nu = \alpha_k$. Since the right-hand side of Eq. (12) is a continuous function, the solution θ is also continuous and can be evaluated at any point.

Table 1 Temperature distribution: $\theta_A = 0.5$, $\theta_B = 1.0$, $\tau_W = 1.0$

Model 1 $\alpha_1 = 1.0$, $\alpha_2 = 0.5$				Model 2 $\alpha_1 = 0.5$, $\alpha_2 = 1.0$			
$\bar{\eta}$	$I = 3$	$I = 13$	Ref. 4	$\bar{\eta}$	$I = 3$	$I = 13$	Ref. 4
−1.0	0.74234	0.74093	0.7408	−1.0	0.75609	0.75447	0.7544
−0.8	0.77314	0.77266	0.7726	−0.8	0.78471	0.78408	0.7841
−0.4	0.81492	0.81482	0.8148	−0.4	0.82519	0.82497	0.8250
0.0	0.84836	0.84840	0.8484	0.0	0.85856	0.85852	0.8585
+0.4	0.87790	0.87805	0.8781	+0.4	0.88864	0.88875	0.8888
+0.8	0.90629	0.90661	0.9066	+0.8	0.91792	0.91829	0.9183
+1.0	0.92272	0.92341	0.9235	+1.0	0.93500	0.93587	0.9359

Table 2 Temperature distribution: $\theta_A = 0.5$, $\theta_B = 1.0$, $\tau_W = 2.0$, model 3 (Ref. 2)

η	$I = 3$	$I = 13$
−1.0	0.72601	0.72311
−0.8	0.76287	0.76186
−0.4	0.81186	0.81158
0	0.85074	0.85073
+0.4	0.88518	0.88539
+0.8	0.91863	0.91921
+1.0	0.93840	0.93979

Numerical Results

It is often desirable to have a continuous rather than discontinuous solution, such as given by step functions. For example, when the solution is given in a continuous form, the optical thickness (which is a function of temperature) can be calculated as a continuous function rather than the averaged values of two adjacent points. Thus, an attempt has been made to obtain a smooth solution directly from the result of a step solution. The step solution itself clearly has many advantages over other representations for the trial function. One of these is that the evaluation of the right-hand side of the integral equation [Eq. (1)] becomes simple, piecewise analytic, and of closed form. The result of radiative transfer for a plane parallel atmosphere where the spectral absorption coefficient takes the Milne-Eddington type is shown in Tables 1 and 2 as a typical example.

Temperature distributions using the step size of $I = 3$ and $I = 13$ are compared with the numerical calculation[4] for several positions, including the boundary points. The present method provides sufficient accuracy for all cases considered in Ref. 4 (since the accuracy of other cases was essentially the same as those given in the table, no additional comparisons are presented in this Note). The present method is intended to provide useful solutions at the boundaries, as well as at any interior point. Temperature distributions at typical points for the multi-rectangular (picket fence) absorption coefficient, which is used in Ref. 2, are included in Table 2 for small ($I = 3$) and large ($I = 13$) step intervals.

Since the computing time quoted in Ref. 2 is proportional to the square of the total step number (I), the spectral number of the absorption coefficient (N), and the number of iterations (M), the reduction of the step size I is the most important factor for a fast calculation. The present result shows that the continuous solution obtained using a small number of steps (e.g., $I = 3$) provides adequate accuracy in all cases considered. This means that the solution obtained with the least number of intervals can be used as effective initial trial functions for obtaining more detailed and accurate solutions. Although the detailed description of the iteration technique is beyond the scope of this Note, it is important to emphasize that an appropriate iteration method is essential to assure the convergence for solutions of nonlinear integral equations. The linear interpolation method, described in Ref. 2, or similar procedures are some of the examples which provide adequate convergence of an otherwise divergent method.

Conclusions

An accurate continuous solution to a general class of nonlinear integral equations with known boundary conditions is obtained directly from the result of previous step (constant) solutions without appreciable work and computing time. Since the continuous solution with a small number of steps provides an adequate description of the exact solution, it is expected that even faster and more accurate solutions will be obtained if one uses the continuous solutions, which are derived from the step function solutions for a small number of intervals, as initial trial functions.

References

[1] Yoshikawa, K. K., "The Variational Solution by the use of Stepwise Constant Function: I. Linear Case," *AIAA Journal*, Vol. 10, No. 3, March 1972, pp. 343–344.

[2] Yoshikawa, K. K., "An Iterative Solution of an Integral Equation for Radiative Transfer by using Variational Technique," TN D-7292, 1973, NASA.

[3] Yoshikawa, K. K., "Variational Solution to the Radiative Equation by the use of Step Function: II. Extension to Nonlinear Case by Iteration Method," *AIAA Journal*, Vol. 11, No. 1, Jan. 1973, pp. 19–23.

[4] Crosbie, A. L. and Viskanta, R., "Rectangular Model for Nongrey Radiative Transfer," *AIAA Journal*, Vol. 8, No. 11, Nov. 1970, pp. 2055–2057.

Use of Slotted Walls to Reduce Wind-Tunnel Boundary Corrections in Subsonic Flow

A. G. PARKER*
Texas A&M University, College Station, Texas

THE author has been working for some time on basic experimental research into the phenomena of the dynamic stall of helicopter rotors. This work has been conducted using a two-dimensional airfoil oscillating in pitch in the Texas A&M University 7 ft × 10 ft low speed wind tunnel. Initially,[1] a 2-ft chord airfoil was used but it became apparent from this and other work[2–4] that the stall process is dominated by the behavior of the leading edge laminar separation bubble and that pressure and velocity measurements in the vicinity of the bubble would be required for a complete understanding of the stall process. In steady flow the length of the bubble is approximately 2% of the chord making detailed measurements in that region difficult. To alleviate the problem a larger airfoil is required. For the same size tunnel this means larger corrections because of tunnel constraints. These corrections, which are nonlinear for a large model at high angles of attack, can be calculated[5] for steady flow and for unsteady sinusoidal motions with attached flow. No documented calculations of corrections for large amplitude oscillations through stall are available.

Since corrections could not be calculated it was decided that, prior to starting oscillatory tests with a 4 ft chord NACA 0012 airfoil, an investigation should be undertaken into methods of eliminating or at least minimizing the corrections required.

Considerable data are available on the use of slotted and porous walls for the reduction of corrections in transonic tunnels,[6–8] but very little has been done to extend this work to low speed subsonic flow where it should also be possible to reduce both lift interference and blockage corrections with the appropriate porosity distribution.

Received June 19, 1974. This work was sponsored by NASA Ames Research Center under Contract NAS2-7917.

Index category: Subsonic and Transonic Flow.

* Assistant Professor, Aerospace Engineering Department. Member AIAA.

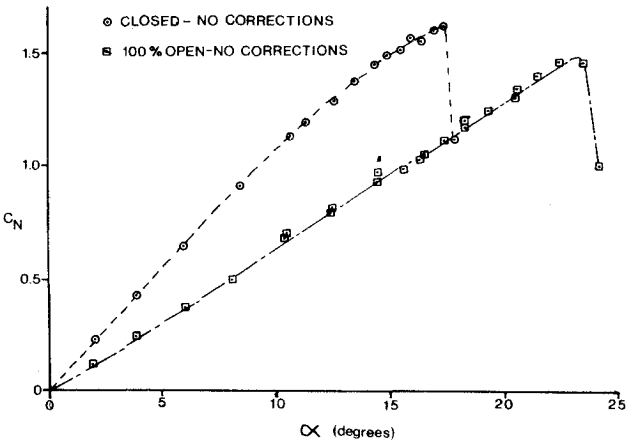

Fig. 1 C_N vs α—**tunnel closed and open without corrections.**

Since corrections can only be calculated for steady flow it was assumed, but not rigorously justified, that if the steady flow corrections could be reduced the unsteady corrections should be similarly reduced. This assumption is probably reasonable at the oscillatory frequencies to be used (1.4Hz max corresponding to a reduced frequency of 0.15).

The solid side walls of the tunnel were therefore removed and replaced with walls having four longitudinal slots the width of which could be varied. The 4 ft chord airfoil was instrumented with ten pressure transducers connected between the upper and lower surfaces. The outputs of these transducers were summed electronically to give normal force (C_N) and pitching moment (C_M) coefficients directly.

Tests were then run at a Reynolds number of 2×10^6 for several angles of attack (α) from zero lift to beyond stall using slot openings from zero to fully open.

Plots of the uncorrected normal force data for the tunnel sidewalls fully closed and fully open are presented in Fig. 1. As can be seen the stall angle in the open case is about 35% greater than in the closed case. Corrections for lift interference and blockage were then applied. For the closed tunnel[5] the corrections for lift interference included terms of order $(c/h)^4$ and blockage terms of order α^2. For the open tunnel results linear corrections were applied.[5,9] Corrected data are plotted in Fig. 2. The two curves are not coincident but this was expected as the corrections for the open sidewalls are linear and only valid for small wings at small angles of attack. The open wall results are therefore overcorrected. The author has considerably more confidence in the results for the closed tunnel and, therefore, these are assumed to be correct.

In Fig. 3 the effect of slot size on $C_N \sim \alpha$ is shown. As the slot size increases from zero, the values of C_N at a given α near

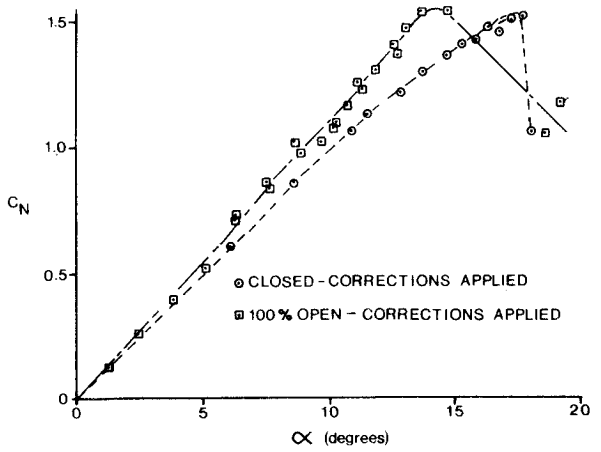

Fig. 2 C_N vs α—**tunnel closed and open with corrections.**